

Quantitative CT Evaluation of Posterior Fossa Volume in Chiari Type II Malformation

Zülküf Akdemir*, Bulut Tuğal

Department of Radiology, Faculty of Medicine, Van Yüzüncü Yıl University, Van, Türkiye

ABSTRACT

To quantitatively evaluate total posterior fossa volume and single-slice volume at the level of the internal acoustic canal on brain CT in patients with Chiari type II malformation and in controls.

In this retrospective single-center study, consecutive patients who underwent brain CT between 2014 and 2018 were identified from the institutional archive using the term “Chiari type II.” Images of all identified cases were re-evaluated. Controls underwent brain CT during the same period and had no abnormality affecting posterior fossa anatomy. Total posterior fossa volume and single-slice internal acoustic canal-level volume were measured on axial noncontrast CT images by using a freehand volume-of-interest tool. Group comparisons, correlation analyses, age-restricted sensitivity analysis, receiver operating characteristic analysis, and age- and sex-adjusted multivariable models were performed.

Eighty participants were included (30 controls and 50 patients with Chiari type II malformation). The Chiari type II group was younger than the control group (median age, 5.5 months [interquartile range {IQR}, 1.0–12.0 months] vs 36.0 months [IQR, 24.0–48.0 months]; $p < 0.001$), whereas sex distribution did not differ ($p = 1.000$). Total posterior fossa volume was significantly lower in the Chiari type II group (34.78 cm³ [IQR, 26.59–58.80] vs 165.80 cm³ [IQR, 159.38–181.52]; $p < 0.001$), as was single-slice internal acoustic canal-level volume (IAC-level single-slice volume) (6.27 cm³ [IQR, 4.17–7.87] vs 9.79 cm³ [IQR, 8.23–11.63]; $p < 0.001$). Total posterior fossa volume correlated positively with age ($r = 0.796$, $p < 0.001$), remained significantly lower in the 1–5-year subgroup ($p < 0.001$), and showed an AUC of 1.000 (95% CI, 1.000–1.000). The corresponding AUC for single-slice internal acoustic canal volume was 0.823 (95% CI, 0.725–0.911). In age- and sex-adjusted models, Chiari type II malformation remained independently associated with lower total posterior fossa volume (adjusted ratio, 0.34; 95% CI, 0.27–0.43; $p < 0.001$) and lower IAC-level single-slice volume (adjusted ratio, 0.78; 95% CI, 0.61–0.99; $p = 0.045$).

Total posterior fossa volume is markedly reduced in Chiari type II malformation and provides stronger group discrimination than single-slice internal acoustic canal-level volume on brain CT.

Keywords: Chiari type II, posterior fossa, volume, computed tomography

Introduction

Chiari type II malformation is a complex developmental malformation characterized by a small posterior fossa, caudal displacement of the cerebellum and brainstem, and a strong association with open spinal dysraphism/myelomeningocele.

Pathophysiologically, the widely cited McLone-Knepper hypothesis proposes that cerebrospinal fluid leakage through the spinal defect reduces distension of the embryonic ventricular system, resulting in an abnormally small posterior fossa. Quantitative neuroimaging studies further suggest that posterior fossa crowding in Chiari II is measurable rather than merely descriptive. (1,2,3)

Chiari malformations are a spectrum of congenital hindbrain anomalies originally described by Chiari and classically divided into types I-IV, although later literature has expanded this framework with

additional variants. (4,5) The pathogenesis of Chiari malformations remains unsettled, and the literature continues to describe multiple, partly overlapping mechanisms rather than a single universally accepted cause. (6,7) Across these mechanisms, posterior fossa constriction due to underdevelopment of the occipital bone, altered cerebrospinal fluid and ventricular distension in the setting of an open neural tube defect, hindbrain overgrowth or disorganized neural development, traction from tethering lesions, and craniocervical instability have all been proposed as contributors to hindbrain descent. (1,5,6)

In children with spina bifida, the effects of Chiari II malformation, together with associated hydrocephalus, are major determinants of neurologic morbidity and long-term outcome. (1) Radiologically, Chiari type II malformation is expressed by a constellation of findings that may include downward herniation of the cerebellum,

*Corresponding Author: Zülküf Akdemir, Yüzüncü Yıl Üniversitesi Tıp Fakültesi, Radyoloji Anabilim Dalı
E-mail: za.radyoloji@hotmail.com

ORCID ID: Zülküf Akdemir: 0000-0001-7958-7235, Bulut Tuğal: 0009-0006-5541-1431

Received: 14.03.2026, Accepted: 12.04.2026

vermis, brainstem, and fourth ventricle, beaked tectum, a hypoplastic or low-lying tentorium, a foreshortened clivus, petrous scalloping, and additional supratentorial and infratentorial abnormalities. (1,2) Because diagnosis and characterization rely on neuroanatomy, MRI has a central role in both clinical assessment and research, and reliable recognition of the essential imaging features is important for consistent phenotyping and management. (2,7)

Morphologic and volumetric studies further reinforce this framework; mesenchymal abnormalities such as a low-lying tentorium, a short clivus, and petrous scalloping have been linked to a small posterior fossa, and CT volumetry in myelomeningocele infants has shown lower posterior cranial fossa volume in more severe hydrocephalic or shunted groups together with an inverse relationship between posterior cranial fossa volume and lateral ventricular volume. (1,6,8) Against this background, explicit CT-based characterization of posterior fossa volume in Chiari type II malformation remains relevant, particularly when the anatomic boundaries and measurement workflow are stated in detail. (2,8)

Accordingly, the aim of the present study was to evaluate posterior fossa volume and single-slice internal acoustic canal-level volume on brain CT in patients with Chiari type II malformation and in controls.

Materials and Methods

Study Design and Ethics: This retrospective single-center study included consecutive patients who underwent brain CT at our institution between 2014 and 2018. The institutional imaging archive and reporting system were searched for the term “Chiari type II,” and all cases documented as Chiari type II malformation were identified, screened for eligibility, and subsequently re-evaluated on imaging.

This study was approved by the Non-Interventional Clinical Research Ethics Committee (decision no. 2026/02-50). The requirement for informed consent was waived owing to the retrospective design.

Study Population and Case Selection: The control group consisted of patients who underwent clinically indicated brain CT examinations during the same period and had no significant intracranial abnormality on imaging. Age and sex were recorded from the institutional

database. Age was standardized to months for statistical analysis.

Control Group Selection and Exclusion

Criteria: Patients were excluded if they had severe hydrocephalus, substantial image artifact (eg, motion or beam-hardening artifact), suboptimal positioning precluding reliable analysis, or poorly delineated posterior fossa boundaries that prevented accurate volumetric measurement. The control group was selected from patients with no anomaly affecting posterior fossa anatomy, no hydrocephalus, no posterior fossa mass or malformation, no cranial bony deformity, and no major developmental anomaly. Control subjects were further excluded if image quality or positioning was inadequate for analysis or if any structural abnormality that could affect posterior fossa measurements was present.

CT Acquisition/Image Dataset: Brain CT examinations were acquired on a 128-slice SOMATOM Definition AS scanner (Siemens Healthineers) using the standard institutional brain CT protocol. Acquisition parameters included a tube voltage of 120 kVp, an effective tube current-time product of 114 mAs, and a section thickness of 4 mm. Images were reconstructed with an Hr36 S3 kernel. Volumetric measurements were performed on axial noncontrast CT images on a syngo.via VB40A workstation (Siemens Healthineers) using the freehand volume-of-interest (VOI) tool.

Only diagnostic-quality brain CT examinations were included in the analysis. All image evaluations and volumetric measurements were performed on CT images displayed in the brain parenchymal window.

Definition of Posterior Fossa Boundaries: For volumetric analysis, the posterior fossa was regarded as the osteodural space containing the hindbrain structures (cerebellum, mesencephalon, pons, and medulla), with boundaries defined by the tentorium cerebelli superiorly, the clivus anteriorly, the petrous bones and petrous ridges anterolaterally, the occipital bone posteriorly, and the foramen magnum/McRae line caudally.

Volumetric Analysis: Volumetric measurements were performed on the workstation using the freehand volume-of-interest (VOI) tool. After the image plane had been appropriately rotated and positioned, the VOI Freehand option was selected from the menu. The first contour was manually traced and completed by double-clicking, after which additional contours were drawn on different image planes of the same image stack to

encompass the target compartment. When necessary, contours were revised using the correction tools available in the contour context menu (eg, the Nudge Tool/Correction Pen). According to the workstation workflow, the freehand VOI was generated to include all voxels located between the manually drawn contours. Inter-slice interpolation was managed through the VOI mini-toolbar displayed at the bottom of the segment; although automatic interpolation was the default mode, contour interpolation could also be used when needed to include the volume between contours. After all required contours had been completed, the Object Creation command was applied to convert the 2-dimensional contours into a 3-dimensional volumetric object. In the VOI Properties window, the output parameters were defined and volume (cm³) was selected as the measurement parameter; the primary recorded variable in the study was the volume expressed in cubic centimeters. In routine application of the freehand VOI method, measurements were typically performed over approximately 50–70 axial slices per case. Contours were drawn separately on each slice, while sagittal and coronal planes were used to confirm the anatomic boundaries. Contour overextension or undercoverage was corrected when necessary. To improve delineation of supra- and infratentorial structures, patient-specific window adjustments were applied before final measurement.

Single-slice Internal Acoustic Canal Measurement: After total posterior fossa volumetry had been completed, single-slice volumetric measurements were performed on a single axial image at the level at which the internal acoustic canals were visualized. For this analysis, the same anatomic boundaries used in the total posterior fossa volume measurements were adopted as reference landmarks. The internal acoustic canal level was selected because it provides a recognizable and relatively consistent anatomic landmark on axial CT images. This single-slice measurement was designed as a sectional surrogate to provide a simplified morphometric estimate at a standardized level and was not intended as a validated replacement for full posterior fossa volumetry.

Reader Information: All volumetric measurements were performed by a radiologist with 12 years of experience. Owing to the characteristic radiologic features of Chiari type II malformation, blinding of the reader to the diagnosis and group allocation was not feasible.

Statistical Analysis: Statistical analyses were performed using IBM SPSS Statistics for Windows, version 25.0 (IBM Corp). Age was converted to months for analysis. Continuous variables are presented as median values with interquartile ranges (IQRs), and categorical variables are presented as counts. Between-group comparisons of continuous variables were performed with the Mann-Whitney U test, and sex distribution was compared with the Fisher exact test. Associations between age and volumetric measurements, as well as between total posterior fossa volume and single-slice volume measured at the level of the internal acoustic canal, were assessed using the Spearman rank correlation coefficient.

Because the Chiari type II group was substantially younger than the control group, a prespecified age-restricted sensitivity analysis was additionally performed in participants aged 1–5 years, using the same between-group comparison methods. The discriminatory performance of total posterior fossa volume and IAC-level single-slice volume for distinguishing Chiari type II malformation from controls was evaluated by receiver operating characteristic (ROC) analysis. The area under the curve (AUC) and corresponding 95% confidence intervals (CIs) were calculated, and optimal cutoff values were determined by the maximum Youden index; sensitivity and specificity were then derived for these thresholds.

To examine whether group differences persisted after adjustment for covariates, separate multiple models were constructed for total posterior fossa volume and IAC-level single-slice volume. For each model, the dependent variable was the natural logarithm of the measured volume, and the independent variables were group, age (per month), and sex. Regression coefficients were exponentiated and are reported as adjusted ratios with 95% CIs. All tests were 2-sided, and $p < 0.05$ was considered to indicate statistical significance.

Results

A total of 80 participants were included, comprising 30 controls and 50 patients with Chiari type II malformation. The demographic and volumetric characteristics of the study cohort are summarized in Table 1. Sex distribution did not differ between the groups (male/female, 14/16 in the control group vs 23/27 in the Chiari type II group; $p = 1.000$). In contrast, the Chiari type II group was significantly younger than the control group (median age, 5.5 months [IQR, 1.0–12.0

Table 1: Demographic characteristics and volumetric measurements of controls and patients with Chiari type II malformation

Variable	Control group	Chiari type II group	p value
Number of participants	30	50	—
Age (months), median (IQR)	36.0 (24.0–48.0)	5.5 (1.0–12.0)	<0.001
Sex, male/female	14/16	23/27	1.000
Total posterior fossa volume (cm ³), median (IQR)	165.80 (159.38–181.52)	34.78 (26.59–58.80)	<0.001
Single-slice volume at the level of the internal acoustic canal (cm ³), median (IQR)	9.79 (8.23–11.63)	6.27 (4.17–7.87)	<0.001

Note: Data are medians, with IQRs in parentheses, unless otherwise indicated. IQR = interquartile range

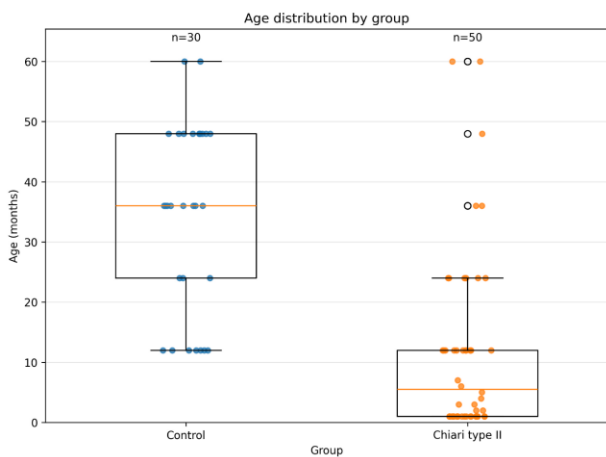


Fig. 1. Age distribution by group
Box-and-whisker plot with individual data points showing age distribution in the control group and in patients with Chiari type II malformation. Ages are expressed in months. Group sample sizes are shown above the plots

months] vs 36.0 months [IQR, 24.0–48.0 months]; $p < 0.001$). The age distribution by group is shown in Figure 1.

Total posterior fossa volume was significantly lower in patients with Chiari type II malformation than in controls (median, 34.78 cm³ [IQR, 26.59–58.80 cm³] vs 165.80 cm³ [IQR, 159.38–181.52 cm³]; $p < 0.001$). Likewise, the single-slice volume measured at the level of the internal acoustic canal was significantly lower in the Chiari type II group than in the control group (median, 6.27 cm³ [IQR, 4.17–7.87 cm³] vs 9.79 cm³ [IQR, 8.23–11.63 cm³]; $p < 0.001$). Representative examples are shown in Figure 2.

Age showed a strong positive correlation with total posterior fossa volume in the overall cohort (Spearman $r = 0.796$, $p < 0.001$). This association remained significant when the groups were

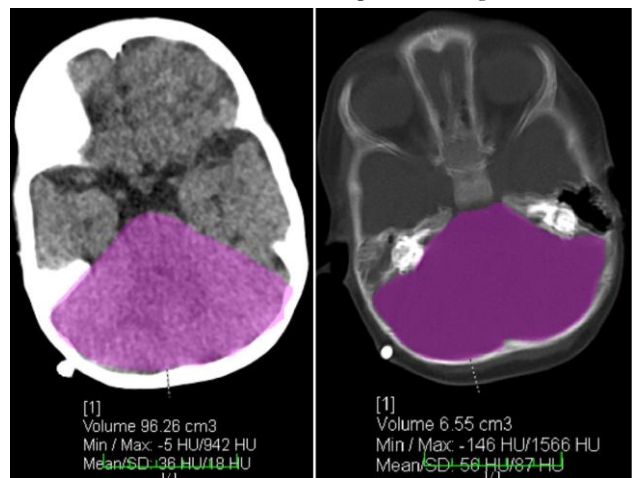


Fig. 2a. Posterior fossa segmentation in a patient with Chiari type II malformation for total posterior fossa volume measurement and single-slice measurement at the level of the internal acoustic canal.

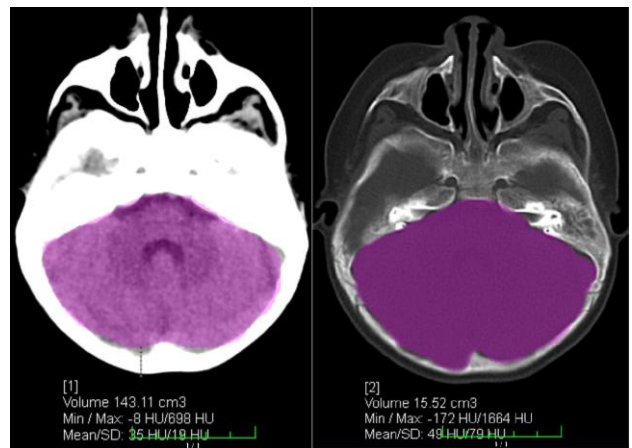


Fig. 2b. Posterior fossa segmentation in a control subject for total posterior fossa volume measurement and single-slice measurement at the level of the internal acoustic canal.

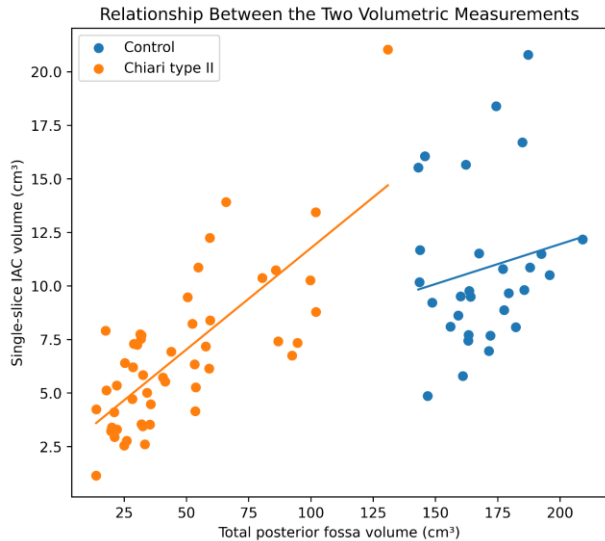


Fig. 3. Scatterplot showing the relationship between total posterior fossa volume and single-slice volume measured at the level of the internal acoustic canal in controls and patients with Chiari type II malformation. Across the overall cohort, the 2 volumetric measurements were positively correlated (Spearman $r = 0.722$, $p < 0.001$). This association remained significant in patients with Chiari type II malformation ($r = 0.671$, $p < 0.001$) but not in controls ($r = 0.219$, $p = 0.246$)

analyzed separately, both in controls ($r = 0.633$, $p < 0.001$) and in patients with Chiari type II malformation ($r = 0.664$, $p < 0.001$). For the single-slice internal acoustic canal measurement, age was also positively correlated with volume in the overall cohort ($\rho = 0.685$, $p < 0.001$). In subgroup analyses, however, this association was not significant in controls ($\rho = -0.138$, $p = 0.467$) but remained significant in the Chiari type II group ($r = 0.649$, $p < 0.001$).

The two volumetric measurements were positively correlated across the entire cohort ($r = 0.722$, $P < 0.001$). When analyzed by group, this relationship was significant in patients with Chiari type II malformation ($r = 0.671$, $p < 0.001$) but not in controls ($r = 0.219$, $p = 0.246$). The relationship between total posterior fossa volume and the single-slice internal acoustic canal measurement is shown in Figure 3.

Given the marked age difference between the groups in the overall cohort, an age-restricted sensitivity analysis was performed in participants aged 1–5 years. This subgroup included 30 controls and 23 patients with Chiari type II malformation. In this restricted analysis, the Chiari type II subgroup remained younger than the control group (median age, 12.0 months [IQR,

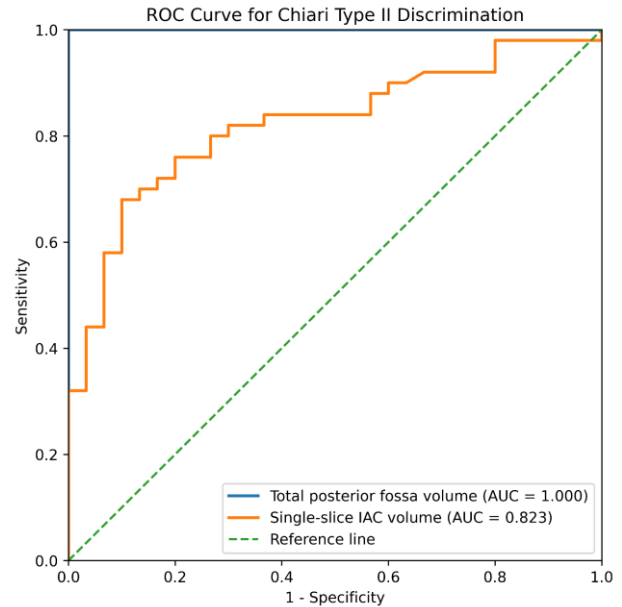


Fig. 4. Receiver operating characteristic curves for total posterior fossa volume and single-slice volume measured at the level of the internal acoustic canal for discrimination of Chiari type II malformation from controls. Total posterior fossa volume showed an AUC of 1.000 (95% CI, 1.000–1.000) in this dataset, whereas the single-slice internal acoustic canal measurement showed lower discriminatory performance (AUC, 0.823; 95% CI, 0.725–0.911)

12.0–24.0 months] vs 36.0 months [IQR, 24.0–48.0 months]; $p = 0.008$). Nevertheless, total posterior fossa volume remained significantly lower in the Chiari type II group than in controls (median, 54.82 cm³ [IQR, 33.94–89.15 cm³] vs 165.80 cm³ [IQR, 159.38–181.52 cm³]; $p < 0.001$). The single-slice internal acoustic canal measurement was also lower in the Chiari type II subgroup (median, 7.74 cm³ [IQR, 6.48–10.55 cm³] vs 9.79 cm³ [IQR, 8.23–11.63 cm³]; $p = 0.034$).

Receiver operating characteristic analysis showed apparent complete separation in this dataset for total posterior fossa volume, with an AUC of 1.000 (95% CI, 1.000–1.000) for distinguishing controls from patients with Chiari type II malformation (Figure 4). In this dataset, a threshold of 130.88 cm³ or less corresponded to 100.0% sensitivity and 100.0% specificity.

By comparison, the single-slice internal acoustic canal measurement showed lower discriminatory performance, with an AUC of 0.823 (95% CI, 0.725–0.911). At a threshold of 7.41 cm³ or less, the single-slice measurement yielded 68.0% sensitivity and 90.0% specificity.

In age- and sex-adjusted models, Chiari type II malformation remained independently associated with lower total posterior fossa volume (adjusted ratio, 0.34; 95% CI, 0.27–0.43; $p < 0.001$). Age was also independently associated with total posterior fossa volume (per month ratio, 1.016; 95% CI, 1.010–1.022; $p < 0.001$), whereas sex was not (female vs male ratio, 0.85; 95% CI, 0.72–1.01; $p = 0.068$). For the single-slice internal acoustic canal measurement, Chiari type II malformation remained associated with lower volume after adjustment, although the magnitude of association was smaller (adjusted ratio, 0.78; 95% CI, 0.61–0.99; $p = 0.045$). Age was independently associated with the single-slice measurement (per month ratio, 1.013; 95% CI, 1.007–1.019; $p < 0.001$), whereas sex was not (female vs male ratio, 0.87; 95% CI, 0.72–1.05; $p = 0.145$).

Together, these results show that total posterior fossa volume demonstrated the strongest separation between groups and maintained a significant association with Chiari type II malformation in both age-restricted and age- and sex-adjusted analyses. The single-slice internal acoustic canal measurement also differed between groups in the overall cohort; however, its discriminatory performance and adjusted effect size were lower than those of total posterior fossa volume.

Discussion

The present study aimed to quantitatively evaluate total posterior fossa volume and single-slice volume at the level of the internal acoustic canal on brain CT images in patients with Chiari type II malformation and in controls. The principal finding of our study was that total posterior fossa volume was significantly lower in patients with Chiari type II malformation than in controls, both in the age-restricted subgroup analysis and in models adjusted for age and sex. This finding is consistent with the established literature indicating that a small posterior fossa plays a central role in the pathophysiology of Chiari type II malformation (1,2,7).

In our study, the median total posterior fossa volume in the Chiari type II group was 34.78 cm³, which was markedly lower than the median value of 165.80 cm³ in the control group. This finding suggests underlying mesenchymal developmental abnormalities and the resulting crowded posterior fossa that characterize Chiari II malformation (1,5). The widely accepted “ventricular distension” hypothesis proposed by McLone and Knepper

holds that cerebrospinal fluid leakage through open spinal dysraphism prevents normal expansion of the embryonic ventricular system, leading to an abnormally small posterior fossa and subsequent hindbrain herniation (1,2,6). Our quantitative findings provide concrete data in support of this hypothesis. Previous studies have shown that mesenchymal abnormalities in Chiari II malformation, including a short clivus, a low-lying tentorium, and petrous bone scalloping, are associated with a small posterior fossa (1). Similarly, Juranek et al. reported reduced total cerebellar volume in patients with spina bifida meningocele/Chiari II and emphasized that posterior fossa crowding in this malformation is not merely descriptive but also measurable (3). By using CT-based volumetry, our study confirms this measurable difference and further supports the concept of reduced posterior fossa volume as a fundamental component of the Chiari II phenotype.

In addition to total posterior fossa volume, we also evaluated a single-slice volumetric measurement obtained at the level of the internal acoustic canal. Although this parameter was also significantly lower in the Chiari type II group than in controls, its discriminatory performance (AUC, 0.823) was inferior to that of total posterior fossa volume (AUC, 1.000). This finding suggests that a single section may not fully capture the global volumetric reduction within the complex three-dimensional anatomy of the posterior fossa. Whereas total posterior fossa volume more comprehensively reflects the overall morphologic impact of this malformation, the measurement obtained at the internal acoustic canal level primarily represents a sectional surrogate at a specific anatomic landmark. Nevertheless, the fact that this simple and rapid measurement was still able to demonstrate a difference between groups implies that posterior fossa narrowing may extend broadly along the craniocaudal axis. To our knowledge, this single-slice measurement has not been described in detail previously and therefore represents a potentially original aspect of our study; however, its diagnostic accuracy and clinical utility require further investigation. Accordingly, this single-slice measurement should be regarded as an exploratory sectional surrogate obtained at a recognizable anatomic landmark rather than as a validated alternative to full volumetric assessment.

In our study, a strong positive correlation was observed between age and total posterior fossa volume in both the Chiari type II and control groups. This was an expected finding, reflecting

ongoing cranial growth during childhood, and is consistent with the work of Chen et al., who modeled the normal growth trajectory of posterior fossa volume during the fetal period (9). These findings suggest that, although the posterior fossa remains developmentally small in Chiari II malformation, it retains some capacity for growth with age. However, the persistence of the absolute volumetric difference between groups even after age-adjusted analyses indicates that growth in the Chiari II group remains below the normal developmental trajectory. This observation supports the concept that the basis of the malformation is established during embryonic development and that postnatal growth does not compensate for this primary deficit (6).

Because the diagnosis and characterization of Chiari II malformation rely largely on neuroanatomy, imaging modalities such as MRI and CT play a central role (2,7). Our study demonstrates that CT-based volumetry can provide quantitative evidence of posterior fossa restriction, which is often assessed qualitatively in routine practice. In this dataset, the threshold value of 130.88 cm³ for total posterior fossa volume corresponded to 100% sensitivity and 100% specificity. However, this finding should be interpreted cautiously and should not be regarded as a clinically validated diagnostic threshold. Rather, it reflects sample-specific separation within this cohort and requires confirmation in independent and age-matched datasets. These findings should not be interpreted as advocating CT acquisition for routine evaluation; rather, they reflect morphometric information derived from existing CT datasets. This distinction is particularly important in pediatric populations, in whom radiation exposure remains an important consideration. As emphasized by Geerdink et al., the identification of reliable and reproducible imaging features may improve the evaluation of Chiari II malformation in both clinical and research settings (2).

This study has several limitations. First, its retrospective design inherently imposed constraints on data collection. Second, there was a marked age imbalance between the Chiari type II and control groups, and this represents a major limitation of the study. Because posterior fossa volume showed a strong positive correlation with age, this imbalance is an important source of confounding in the interpretation of between-group volumetric differences. Although this issue was addressed statistically through an age-restricted subgroup analysis and age- and sex-

adjusted models, these approaches do not fully eliminate the possibility of residual confounding. Accordingly, the observed between-group separation should be interpreted with caution, and a prospective study with age- and sex-matched controls would provide more definitive results. Because the control group was selected from clinically imaged patients rather than from a population-based healthy sample, selection bias cannot be excluded. Third, because Chiari type II malformation has characteristic radiologic features, blinding of the interpreting radiologist to the diagnosis was not feasible, which may have introduced observer bias. In addition, all measurements were performed by a single radiologist, and formal inter-observer or intra-observer reproducibility analyses were not performed. Because the freehand VOI method includes manual contouring, the reproducibility of these measurements remains to be established. Finally, this was a single-center study, and multicenter investigations are needed to improve the generalizability of these findings.

References

1. McLone DG, Dias MS. The Chiari II malformation: cause and impact. *Childs Nerv Syst*. 2003; 19: 540-550.
2. Geerdink N, van der Vliet T, Rotteveel JJ, Feuth T, Roeleveld N, Mullaart RA. Essential features of Chiari II malformation in MR imaging: an interobserver reliability study--part 1. *Childs Nerv Syst* 2012; 28: 977-985.
3. Juranek J, Dennis M, Cirino PT, El-Messidi L, Fletcher JM. The cerebellum in children with spina bifida and Chiari II malformation: Quantitative volumetrics by region. *Cerebellum* 2010; 9: 240-248.
4. Azahraa Haddad F, Qaisi I, Joudeh N, et al. The newer classifications of the chiari malformations with clarifications: An anatomical review. *Clin Anat* 2018; 31: 314-322.
5. Nishikawa M, Bolognese PA, Yoshimura M, et al. Chiari Malformation and Hindbrain Descent: Characterization and New Classification Based on Mechanism and Pathogenesis, and Surgical Management. *Neurospine* 2025; 22: 696-712.
6. Shoja MM, Johal J, Oakes WJ, Tubbs RS. Embryology and pathophysiology of the Chiari I and II malformations: A comprehensive review. *Clin Anat* 2018; 31: 202-215.
7. Kuhn J, Weisbrod LJ, Emmady PD. Chiari Malformation Type 2. In: *StatPearls*. Treasure Island (FL): StatPearls Publishing; February 25, 2024.
8. Hashimoto H, Irizato N, Takemoto O, Chiba Y. Intracranial volumetric evaluation in postnatally

repaired myelomeningocele infants. *Childs Nerv Syst* 2024; 40: 2851-2858.

9. Chen SC, Simon EM, Haselgrove JC, et al. Fetal posterior fossa volume: assessment with MR imaging. *Radiology* 2006; 238: 997-1003.